Stability Analyses for Car-following Helly's Model and two of its control schemes ⋆

Oscar A. Rosas-Jaimes * **Luis A. Quezada-Téllez** **
Guillermo Fernández-Anaya ***

* *Facultad de Ciencias de la Electrónica, Benemérita Universidad Autónoma de Puebla, Puebla, México (e-mail: oscar.rosasj@)correo.buap.mx.*
** *Departamento de Física y Matemáticas, Universidad Iberoamericana, México, D. F., México (e-mail: alquezada@ciencias.unam.mx)*
*** *Departamento de Física y Matemáticas, Universidad Iberoamericana, México, D. F., México (e-mail: guillermo.fernandez@ibero.mx)*

Abstract: This paper takes a previous manuscript in which the car-following Helly's model was used to design two different control schemes: one Proportional-Integral regulator and an Optimal Control scheme. In this document, we are presenting the stability analysis of the car-following model as well as the stability analyses of those control designs. Of course, the stability character of all of those approaches are confirmed, but the way in which they are obtained are quite interesting due to the results and implications obtained.

Keywords: Stability Analysis; Lyapunov Functions; Car-following Models; Helly's Model; PI-Controller; Optimal Control.

1. INTRODUCTION

This paper is totally based on the work by (Rosas-Jaimes et al., 2015). This time, we take advantage of the space and the opportunity to develop the corresponding stability analyses of all the models and control designs presented in that manuscript in order to make a complete framework of such schemes.

In this way, this present document shows the ways in which those expressions are stable, but also generalizes those results and points out details about the involved parameters and the physical approaches in which they are applied.

The theoretical background, in this case, is the same as for the paper of (Rosas-Jaimes et al., 2015) which studies Helly's Car-Following Model (Helly , 1959) as an extension of Pipes' Car-Following Model (Pipes, 1953).

Those two models were presented and analyzed by its respective authors. However, we present here Lyapunov stability approaches for both of them, confirming the stable nature of these two models under realistic assumptions, and then we span this idea to the Proportional–Integral Control and the Optimal plus Proportional–Integral Regulator developed and presented in (Rosas-Jaimes et al., 2015).

Such control schemes have not been taken into account in literature as far as we know, and the same can be said about their Lyapunov-type stability analyses.

⋆ This research has been supported by PROED fonds.

This paper is organized as follows: Section 2 presents a brief description of Pipes' and Helly's Car-Following Models. Details about such models can be found in (Rosas-Jaimes et al., 2015), as mentioned. Section 3 is the main purpose of this text, and herein we develop the stability analyses for the two models and for the two control approaches already mentioned. As we will show, these analyses give deeper insights about the conditions and quantities under which these expressions are realistically stable, giving support to automotive applications, for example. Section 4 contains the main conclusions of this communication.

2. DESCRIPTION OF MODELS AND CONTROL DESIGNS

Car-following models represent systems formed by two moving vehicles, one in the front and another behind, translating in a single lane, with $v_L(t)$ as the velocity of the car in front (leader) and $v_f(t)$ as the velocity of the car in the back (follower), assuming that passings are not allowed (Treiber et al., 2000).

Since more than sixty years, several models trying to represent such a phenomena have arisen, being a simple and intuitive model proposed by (Pipes, 1953) one of the first to be known. Pipes' Model has the following expression

$$\frac{dv_f(t)}{dt} = \lambda \left[v_L(t) - v_f(t) \right] \tag{1}$$

where λ is a sensitivity parameter, related with the reactive behavior of the driver in the follower car, a quantity considered as $\lambda \in [0, 1]$.

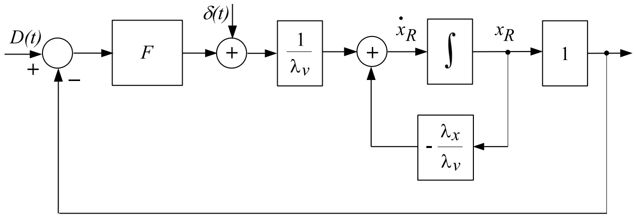

Fig. 1. Block diagram for output feedback applied to Helly's model based on (3)

Helly (1959) extends Pipes' model introducing a term that takes into account the relative position of the vehicles

$$\frac{dv_f(t)}{dt} = \lambda_v\left[v_L(t) - v_f(t)\right] + \\ + \lambda_x\left[x_L(t) - x_f(t) - D(t)\right] \quad (2)$$

In equation (2) λ_v is the same sensitivity parameter as in Pipes' equation (1) that affects the difference of velocities, meanwhile λ_x is a parameter for the additional term of the difference between the leader's position $x_L(t)$ and the follower's position $x_f(t)$, which is in turn affected by a desired distance $D(t)$. This last term adjusts the driver's response in such a way that it depends on the relative distance $x_R(t) = x_L(t) - x_f(t)$ and not only on the relative velocity $v_R(t) = v_L(t) - v_f(t)$. As for the case of Pipes' model, for Helly's model $\lambda_v \in [0, 1]$ and $\lambda_x \in [0, 1]$. An alternative expression of (2) is as follows

$$\dot{x}_R(t) = -\frac{\lambda_x}{\lambda_v}\left[x_R(t)\right] + \frac{1}{\lambda_v}\left[\dot{v}_f(t) + \lambda_x D(t)\right] \quad (3)$$

Equation (2) can also be written in a matrix form

$$\begin{bmatrix} \dot{v}_f \\ \dot{x}_R \end{bmatrix} = \begin{bmatrix} -\lambda_v & \lambda_x \\ -1 & 0 \end{bmatrix} \begin{bmatrix} v_f \\ x_R \end{bmatrix} + \begin{bmatrix} \lambda_v & -\lambda_x \\ 1 & 0 \end{bmatrix} \begin{bmatrix} v_L \\ D \end{bmatrix} \quad (4)$$

with the state $[v_f \;\; x_R]^T$ and an output expression

$$y = [\,0\;\;1\,] \begin{bmatrix} v_f \\ x_R \end{bmatrix} \quad (5)$$

See (Rosas-Jaimes et al., 2015) for details.

Because Helly's model is a more complete approach than Pipes', and still preserves a simple and intuitive understanding of the represented phenomena, it is preferred to be used for developing control designs on it.

(Rosas-Jaimes et al., 2015) have proposed an output feedback control based on Equation (3) as depicted in Figure 1, with a control function F

$$F = k\frac{s+a}{s} = k + \frac{ka}{s} \quad (6)$$

Another control scheme suggested in (Rosas-Jaimes et al., 2015) is an Optimal Control with a Proportional plus Integral feedback as shown in Figure 2 with a state control matrix K

$$K = R^{-1}B^T P = \\ = \begin{bmatrix} \dfrac{-2\lambda_x}{\lambda_v+\lambda_x} + \dfrac{2\sqrt{\lambda_v^2+\lambda_v\lambda_x+\lambda_x^2}}{\lambda_v+\lambda_x} & \dfrac{\sqrt{2}}{2}\lambda_x \\ \dfrac{\lambda_v}{\lambda_v+\lambda_x} - \dfrac{\sqrt{\lambda_v^2+\lambda_v\lambda_x+\lambda_x^2}}{\lambda_v+\lambda_x} & 0 \end{bmatrix} \quad (7)$$

And matrices A, B, C, and R defined as

$$A = \begin{bmatrix} -\lambda_v & \lambda_x \\ -1 & 0 \end{bmatrix} \qquad B = \begin{bmatrix} \lambda_v & -\lambda_x \\ 1 & 0 \end{bmatrix}$$

$$C = [\,0\;\;1\,] \qquad R = \begin{bmatrix} \lambda_v/2 & 0 \\ 0 & \lambda_x \end{bmatrix}$$

Matrix P is an important stability factor as for the design of this regulator as for the analysis that will be performed in the next section, with the properties of being symmetric and positive definite.

$$P = \begin{bmatrix} \dfrac{-\lambda_v}{\lambda_v+\lambda_x} + \dfrac{\sqrt{\lambda_v^2+\lambda_v\lambda_x+\lambda_x^2}}{\lambda_v+\lambda_x} & 0 \\ 0 & \dfrac{\sqrt{2}}{2}\lambda_v \end{bmatrix} \quad (8)$$

See (Rosas-Jaimes et al., 2015) for details about these designs.

3. STABILITY ANALYSES

3.1 Pipes' Model Stability

We begin our analyses with Pipes' Model (1), expressed as in equation (9)

$$\frac{dv_f}{dt} = -\lambda v_f + \lambda v_L \quad (9)$$

Let $V_p(v_f)$ a Lyapunov function candidate such as

$$V_p(v_f) = \frac{1}{2}v_f^2 \quad (10)$$

Its time derivative is given by

$$\dot{V}_p(v_f) = v_f\frac{dv_f}{dt} = v_f\left(-\lambda v_f + \lambda v_L\right) \quad (11)$$

Equation (11) can be rewritten as Equation (12)

$$\dot{V}_p(v_f) = \lambda v_f\left(v_L - v_f\right) \le 0 \quad (12)$$

Equation (12) states that Pipes' Model is stable.

This last statement is true when $v_f \ge v_L$. This happens when the follower vehicle is getting closer to the leader vehicle, and then a decreasing behavior in v_f is observed as $v_f \to v_L$. A steady state is reached when $v_f = v_L$.

In the possible case in which v_L has a larger value than v_f, then the leader vehicle is leaving behind the follower vehicle, and their separation increases without limit, unless the relation between these velocities varies in the opposite situation.

3.2 Helly's Model Stability

Let Helly's Model be in the state form (4). And let $V_H(v_f, x_R)$ be a Lyapunov candidate function as in Equation (13)

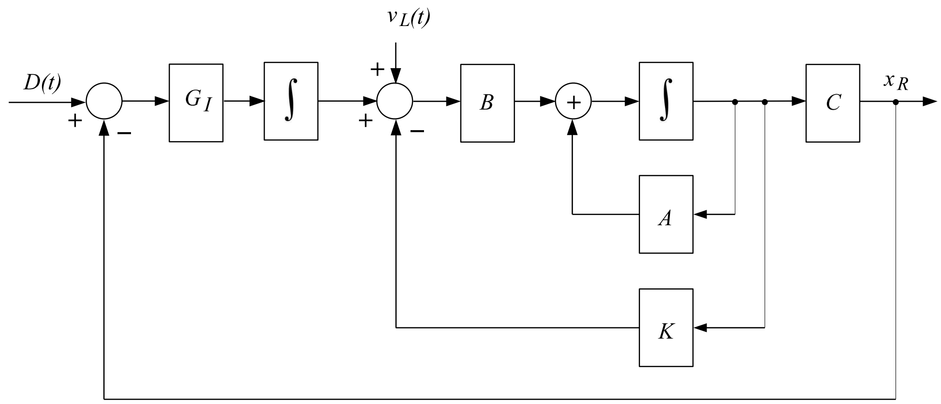

Fig. 2. Block diagram for optimal-integral control for Helly's model

$$V_H(v_f, x_R) = [\, v_f \;\; x_R \,] \begin{bmatrix} p_{11} & p_{12} \\ p_{12} & p_{22} \end{bmatrix} \begin{bmatrix} v_f \\ x_R \end{bmatrix} \quad (13)$$

For a symmetric and positive definite matrix P.

Derivative of $V_H(v_f, x_R)$ is given by Equation (14)

$$\dot{V}_H(v_f, x_R) = [\, v_f \;\; x_R \,] \begin{bmatrix} p_{11} & p_{12} \\ p_{12} & p_{22} \end{bmatrix} \begin{bmatrix} \dot{v}_f \\ \dot{x}_R \end{bmatrix} + + [\, \dot{v}_f \;\; \dot{x}_R \,] \begin{bmatrix} p_{11} & p_{12} \\ p_{12} & p_{22} \end{bmatrix} \begin{bmatrix} v_f \\ x_R \end{bmatrix} \quad (14)$$

When substituting time derivative parts in Equation (14), Equation (15) is obtained

$$\begin{aligned} \dot{V}_H(v_f, x_R) = {} & [\, v_f \;\; x_R \,] \begin{bmatrix} p_{11} & p_{12} \\ p_{12} & p_{22} \end{bmatrix} \cdot \\ & \cdot \left(\begin{bmatrix} -\lambda_v & \lambda_x \\ -1 & 0 \end{bmatrix} \begin{bmatrix} v_f \\ x_R \end{bmatrix} + \begin{bmatrix} \lambda_v & -\lambda_x \\ 1 & 0 \end{bmatrix} \begin{bmatrix} v_L \\ D \end{bmatrix} \right) + \\ & + \left([\, v_f \;\; x_R \,] \begin{bmatrix} -\lambda_v & -1 \\ \lambda_x & 0 \end{bmatrix} + [\, v_L \;\; D \,] \begin{bmatrix} \lambda_v & 1 \\ -\lambda_x & 0 \end{bmatrix} \right) \cdot \\ & \cdot \begin{bmatrix} p_{11} & p_{12} \\ p_{12} & p_{22} \end{bmatrix} \begin{bmatrix} v_f \\ x_R \end{bmatrix} \end{aligned} \quad (15)$$

By performing operations, then Equation (15) can be written as Equation (16) shows in the following developed expression

$$\begin{aligned} \dot{V}_H(v_f, x_R) = 2\, [& \lambda_v \,(v_L - v_f)\, v_f p_{11} + \\ & + \lambda_v \,(v_L - v_f)\, x_R p_{12} + \\ & + \lambda_x \,(x_R - D)\, v_f p_{11} + \\ & + \lambda_x \,(x_R - D)\, x_R p_{12} + \\ & + (v_L - v_f)\, v_f p_{12} + \\ & + (v_L - v_f)\, x_R p_{22}] \end{aligned} \quad (16)$$

When grouping by p_{ij} elements, then Equation (16) is rewritten as it is presented by Equation (17) in the following

$$\begin{aligned} \dot{V}_H(v_f, x_R) = {} & 2\, [\lambda_v \,(v_L - v_f) + \lambda_x \,(x_R - D)]\, v_f p_{11} + \\ & + 2\, \{ [\lambda_v \,(v_L - v_f) + \lambda_x \,(x_R - D)]\, x_R + \\ & + (v_L - v_f)\, v_f \}\, p_{12} + \\ & + 2\, (v_L - v_f)\, x_R p_{22} \end{aligned} \quad (17)$$

In order to take into account the condition of symmetry and positive definitiveness of P, let $p_{11} = v_f$, $p_{12} = 0$ and $p_{22} = x_R$. Then $\dot{V}_H(v_f, x_R)$ becomes

$$\begin{aligned} \dot{V}_H(v_f, x_R) = {} & 2\, [\lambda_v \,(v_L - v_f) + \lambda_x \,(x_R - D)]\, v_f^2 + \\ & + 2\, (v_L - v_f)\, x_R^2 \leq 0 \end{aligned} \quad (18)$$

and then Helly's Model is stable.

Equation (18) is true if $v_f \geq v_L$ and $D \geq x_R$. This situation occurs when the follower vehicle is getting closer to the leader. Similar to the case of Pipes' Model, if the velocity of the leader is larger than the velocity of the follower, then this last one is left behind and the distance x_R is increased without limit.

3.3 Output Feedback Control Stability

Helly's Model taken as Equation (3) can be properly modified in order to take the term where $\dot{v}_f$ and D appear as inputs and then be expressed as in Equation (19) where a disturbance $\delta(t)$ is also included

$$\dot{x}_R(t) = -\frac{\lambda_x}{\lambda_v}\, [x_R(t)] + \frac{1}{\lambda_v}\, [u(t) + \delta(t)] \quad (19)$$

In (Rosas-Jaimes et al., 2015) a control input $u(t)$ is obtained by designing a proportional plus integral output feedback for regulating the distance x_R, as stated by the following Equation (20)

$$u(t) = ka \int_{to}^{t1} (D - x_R)\, dt + k\, (D - x_R) \quad (20)$$

where D is a safety distance between cars that appears as a lower limit to x_R, and k and a are convenient design constants. Let V_{FH} a Lyapunov candidate function for analyzing the stability of this output feedback approach in Helly's model, with an expression (21) as follows

$$V_{FH} = \frac{1}{2} x_R^2 \quad (21)$$

Then, its time derivative is given as Equation (22) presents in the following:

$$\dot{V}_{FH} = x_R \dot{x}_R \tag{22}$$

By proper substitution of Equations (19) and (20) in Equation (22):

$$\begin{aligned} \dot{V}_{FH} = x_R \Big\{ & -\frac{\lambda_x}{\lambda_v} x_R + \\ & + \frac{1}{\lambda_v} \left[ka \int_{to}^{t1} (D - x_R)\, dt + k\,(D - x_R) \right] + \\ & + \frac{1}{\lambda_v} \Big[\delta(t) \Big] \Big\} \end{aligned} \tag{23}$$

This expression of $\dot{V}_{FH}$ can be written in the alternate version given by Equation (24)

$$\begin{aligned} \dot{V}_{FH} = & -\frac{\lambda_x}{\lambda_v} x_R^2 - \frac{x_R}{\lambda_v} ka \int_{t_0}^{t_1} (x_R - D)\, dt - \\ & - \frac{x_R}{\lambda_v} k\,(x_R - D) - \frac{x_R}{\lambda_v} \delta(t) \leq 0 \end{aligned} \tag{24}$$

showing up that this output feedback control is stable.

Equation (24) is true if $x_R \geq D$ and $\delta(t)$ is bounded. The first statement is the same as that mentioned for Pipes' and Helly's models in the sense that the follower vehicle approaches to the leader vehicle, making $x_R \to D$.

Disturbance $\delta(t)$ must be bounded as Equation (25) states

$$\delta(t) \leq \lambda_x x_R + ka \int_{t_0}^{t_1} (x_R - D)\, dt + k\,(x_R - D) \tag{25}$$

Adding and substracting $\lambda_x D$ and taking absolute values on (25) results in

$$\begin{aligned} |\delta(t)| \leq & \lambda_x |x_R - D| + ka \left| \int_{t_0}^{t_1} (x_R - D)\, dt \right| + \\ & + k|x_R - D| + \lambda_x D \\ \leq & \lambda_x |x_R - D| + ka|x_R - D| \max(t_1 - t_0) \\ & + k|x_R - D| + \lambda_x D \end{aligned} \tag{26}$$

And then

$$|\delta(t)| \leq [\lambda_x + ka \max(t_1 - t_0) + k]\, |x_R - D| + \lambda_x D \tag{27}$$

In this way, disturbance $\delta(t)$ is a varying quantity, instead of a constant value, for $x_R > D$. If $x_R = D$ then

$$|\delta(t)| \leq \lambda_x D \tag{28}$$

3.4 Optimal Control Scheme Stability

A second control design presented in (Rosas-Jaimes et al., 2015) is an Optimal Linear control with a Proportional–Integral regulator (see Figure 2). This scheme takes on leader's velocity v_L as a disturbance to Helly's description of the follower vehicle, which affects its behavior. For this design, Equations (4) and (5) were used.

Let $u(t)$ the control input to Helly's scheme in such a way that:

$$u(t) = -K \begin{bmatrix} v_f \\ x_R \end{bmatrix} + \begin{bmatrix} v_L \\ G_I \int_{t_0}^{t_1} (D - x_R) dt \end{bmatrix} \tag{29}$$

In this manner, from Equations (4) and (29):

$$\begin{aligned} \begin{bmatrix} \dot{v}_f \\ \dot{x}_R \end{bmatrix} &= A \begin{bmatrix} v_f \\ x_R \end{bmatrix} + Bu(t) = \\ &= A \Bigg\{ (I + K) \begin{bmatrix} v_f \\ x_R \end{bmatrix} - \\ & - \begin{bmatrix} v_L \\ G_I \int_{t_0}^{t_1} (D - x_R) dt \end{bmatrix} \Bigg\} \end{aligned} \tag{30}$$

Let $V_{HO}(v_f, x_R)$ be a candidate Lyapunov function with a similar expression as in Equation (13). Because P is symmetric, then the time derivative of $V_{HO}(v_f, x_R)$ is

$$\dot{V}_{HO}(v_f, x_R) = 2 \,[\, v_f \;\; x_R \,]\, P \begin{bmatrix} \dot{v}_f \\ \dot{x}_R \end{bmatrix} \tag{31}$$

Substitution of (30) in (31) is written as:

$$\begin{aligned} \dot{V}_{HO}(v_f, x_R) = 2 \,[\, v_f \;\; x_R \,]\, PA \Bigg\{ & (I + K) \begin{bmatrix} v_f \\ x_R \end{bmatrix} - \\ & - \begin{bmatrix} v_L \\ G_I \int_{t_0}^{t_1} (D - x_R) dt \end{bmatrix} \Bigg\} \end{aligned} \tag{32}$$

Specific forms of P and K are taken from (Rosas-Jaimes et al., 2015) as mentioned, then

$$\begin{aligned} \dot{V}_{HO} = & 2 \,[\, v_f \;\; x_R \,] \cdot \\ & \cdot \begin{bmatrix} \frac{-\lambda_v}{\lambda_v + \lambda_x} + \frac{\sqrt{\lambda_v^2 + \lambda_v \lambda_x + \lambda_x^2}}{\lambda_v + \lambda_x} & 0 \\ 0 & \frac{\sqrt{2}}{2} \lambda_v \end{bmatrix} \begin{bmatrix} -\lambda_v & \lambda_x \\ -1 & 0 \end{bmatrix} \cdot \\ & \cdot \Bigg\{ \Bigg(\begin{bmatrix} 1 & 0 \\ 0 & 1 \end{bmatrix} + \\ & + \begin{bmatrix} \frac{-2\lambda_x}{\lambda_v + \lambda_x} + \frac{2\sqrt{\lambda_v^2 + \lambda_v \lambda_x + \lambda_x^2}}{\lambda_v + \lambda_x} & \frac{\sqrt{2}}{2} \lambda_x \\ \frac{\lambda_v}{\lambda_v + \lambda_x} - \frac{\sqrt{\lambda_v^2 + \lambda_v \lambda_x + \lambda_x^2}}{\lambda_v + \lambda_x} & 0 \end{bmatrix} \Bigg) \begin{bmatrix} v_f \\ x_R \end{bmatrix} - \\ & - \begin{bmatrix} v_L \\ G_I \int_{t_0}^{t_1} (D - x_R) dt \end{bmatrix} \Bigg\} \end{aligned} \tag{33}$$

Equation (33) can be briefly written as:

$$\dot{V}_{HO} = [\, v_f \;\; x_R \,]\, S \begin{bmatrix} v_f \\ x_R \end{bmatrix} - [\, v_f \;\; x_R \,]\, T \tag{34}$$

where basically, matrix S contains the optimal control part and T contains the PI and the perturbation v_L elements. S is a square matrix included in a quadratic form, but matrix T is not. Then it turns out necessary to fully develop the scalar function of $\dot{V}_{HO}$.

From the terms in (37) it is possible to observe and probe that the quantity indicated by (37a) is positive, independently of the actual values of v_f, λ_v and λ_x. This quantity is a factor affecting the rest of the terms in (37), Performing operations and grouping properly:

$$\dot{V}_{HO} = \frac{2v_f^2}{(\lambda_v+\lambda_x)^2}\left\{\lambda_v\left[(\lambda_v+3\lambda_x)\sqrt{\lambda_v^2+\lambda_v\lambda_x+\lambda_x^2}-2\lambda_v\lambda_x\right]-(\lambda_v+\lambda_x)^3\right\}+$$
$$+\frac{2v_f x_R}{(\lambda_v+\lambda_x)^2}\left\{\lambda_x\left[\lambda_v\left(\frac{\sqrt{2}}{2}\lambda_v-2\right)-\left(\frac{\sqrt{2}}{2}\lambda_x+2\right)\sqrt{\lambda_v^2+\lambda_v\lambda_x+\lambda_x^2}\right]\right\}-$$
$$-\frac{2v_f}{\lambda_v+\lambda_x}\frac{\sqrt{2}}{2}\lambda_v x_R\left(\lambda_v-\lambda_x+2\sqrt{\lambda_v^2+\lambda_v\lambda_x+\lambda_x^2}\right)-$$
$$-\frac{2v_f}{\lambda_v+\lambda_x}\left[\lambda_v^2 v_L-\lambda_v v_L\sqrt{\lambda_v^2+\lambda_v\lambda_x+\lambda_x^2}+\lambda_x\left(\sqrt{\lambda_v^2+\lambda_v\lambda_x+\lambda_x^2}-\lambda_v\right)\left(G_I\int_{t_0}^{t_1}Ddt-G_I\int_{t_0}^{t_1}x_R dt\right)\right]+$$
$$+\sqrt{2}\lambda_v v_L x_R-\lambda_v\lambda_x x_R^2 \tag{35}$$

Equation (35) can be reorganized by sign and by factorizing through v_L, v_f and x_R:

$$\dot{V}_{HO} = \frac{2v_f}{(\lambda_v+\lambda_x)^2}\left\{v_f\left[\lambda_v(\lambda_v+3\lambda_x)\sqrt{\lambda_v^2+\lambda_v\lambda_x+\lambda_x^2}\right]+x_R\left[\frac{\sqrt{2}}{2}\lambda_v^2\lambda_x+\frac{\sqrt{2}}{2}\lambda_v\lambda_x(\lambda_v+\lambda_x)\right]\right\}+$$
$$+\frac{2v_f}{\lambda_v+\lambda_x}\left\{v_L\left[\lambda_v\sqrt{\lambda_v^2+\lambda_v\lambda_x+\lambda_x^2}\right]+\lambda_v\lambda_x G_I\int_{t_0}^{t_1}Ddt+\lambda_x\sqrt{\lambda_v^2+\lambda_v\lambda_x+\lambda_x^2}G_I\int_{t_0}^{t_1}x_R dt\right\}-$$
$$-\frac{2v_f}{(\lambda_v+\lambda_x)^2}\left\{v_f\left[2\lambda_v^2\lambda_x+(\lambda_v+\lambda_x)^3\right]+x_R\left[2\lambda_v\lambda_x+\left(\frac{\sqrt{2}}{2}\lambda_x+2\right)\lambda_x\sqrt{\lambda_v^2+\lambda_v\lambda_x+\lambda_x^2}+\right.\right.$$
$$\left.\left.+\frac{\sqrt{2}}{2}\lambda_v^2(\lambda_v+\lambda_x)+\sqrt{2}\lambda_v(\lambda_v+\lambda_x)\sqrt{\lambda_v^2+\lambda_v\lambda_x+\lambda_x^2}\right]+x_R^2\left[\frac{1}{2v_f}\lambda_v\lambda_x(\lambda_v+\lambda_x)^2\right]\right\}-$$
$$-\frac{2v_f}{\lambda_v+\lambda_x}\left\{v_L\left[\lambda_v^2\right]+\lambda_x\sqrt{\lambda_v^2+\lambda_v\lambda_x+\lambda_x^2}G_I\int_{t_0}^{t_1}Ddt+\lambda_v\lambda_x G_I\int_{t_0}^{t_1}x_R dt\right\} \tag{36}$$

From Equation (36) it is possible to group the terms in order to achieve the following useful expression:

$$\dot{V}_{HO} = \frac{2v_f}{(\lambda_v+\lambda_x)^2}\cdot \tag{37a}$$
$$\cdot\left\{v_f\left[\lambda_v(\lambda_v+3\lambda_x)\sqrt{\lambda_v^2+\lambda_v\lambda_x+\lambda_x^2}-2\lambda_v^2\lambda_x-(\lambda_v+\lambda_x)^3\right]+\right. \tag{37b}$$
$$+x_R\left[\frac{\sqrt{2}}{2}\lambda_v^2\lambda_x+\frac{\sqrt{2}}{2}\lambda_v\lambda_x(\lambda_v+\lambda_x)-\right.$$
$$\left.-2\lambda_v\lambda_x-\left(\frac{\sqrt{2}}{2}\lambda_x+2\right)\lambda_x\sqrt{\lambda_v^2+\lambda_v\lambda_x+\lambda_x^2}-\frac{\sqrt{2}}{2}\lambda_v^2(\lambda_v+\lambda_x)-\sqrt{2}\lambda_v(\lambda_v+\lambda_x)\sqrt{\lambda_v^2+\lambda_v\lambda_x+\lambda_x^2}\right]+ \tag{37c}$$
$$+v_L\left[\lambda_v\sqrt{\lambda_v^2+\lambda_v\lambda_x+\lambda_x^2}-\lambda_v^2\right]- \tag{37d}$$
$$-x_R^2\left[\frac{1}{2v_f}\lambda_v\lambda_x(\lambda_v+\lambda_x)^2\right]+ \tag{37e}$$
$$\left.+\lambda_x\left(\lambda_v-\sqrt{\lambda_v^2+\lambda_v\lambda_x+\lambda_x^2}\right)G_I\int_{t_0}^{t_1}(D-x_R)\,dt\right\} \tag{37f}$$

and therefore the sign of $\dot{V}_{HO}$ is rather dependent on the relations of such terms.

The term in brackets affected by v_L in (37b) and the term in brackets affected by x_R in (37c) are non-positive. One easy manner to show this fact is by means of graphical representations for each of such terms. See Figures 3 and 4.

The term in brackets affected by x_R^2 in (37e) including its negative sign is a non-positive quantity also.

In order to stablish the sign of the terms of (37d) and (37f), sum both indicated terms to achieve the expression (38):

$$v_L\left[\lambda_v\sqrt{\lambda_v^2+\lambda_v\lambda_x+\lambda_x^2}-\lambda_v^2\right]+$$
$$+\lambda_x\left(\lambda_v-\sqrt{\lambda_v^2+\lambda_v\lambda_x+\lambda_x^2}\right)G_I\int_{t_0}^{t_1}(D-x_R)\,dt=$$
$$=\left(\lambda_v-\sqrt{\lambda_v^2+\lambda_v\lambda_x+\lambda_x^2}\right)\cdot \tag{38a}$$
$$\cdot\left[\lambda_x G_I\int_{t_0}^{t_1}(D-x_R)\,dt-v_L\lambda_v\right] \tag{38b}$$

Quantity (38a) is non-positive.

By defintion $x_R \geq D$ and then the integration is non-positive. Therefore, factor (38b) is also non-positive.

Because (38a) and (38b) are each one of them non-positive, then

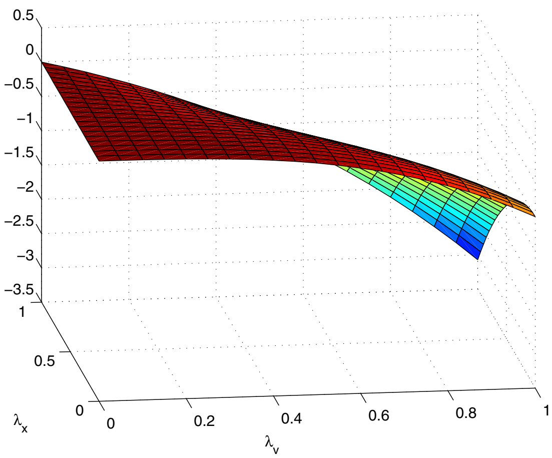

Fig. 3. Plotted representation of Function (37b).

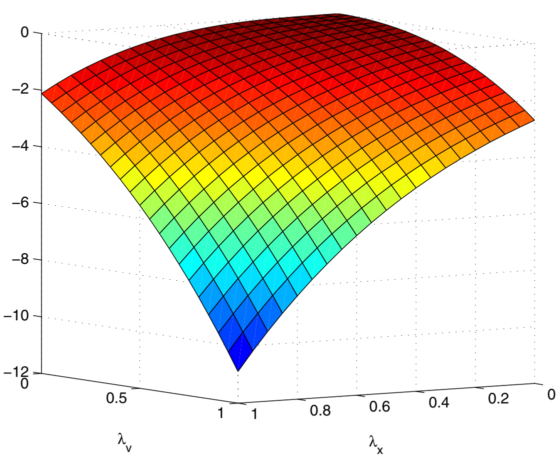

Fig. 4. Plotted representation of Function (37c).

$$\left(\lambda_v - \sqrt{\lambda_v^2 + \lambda_v\lambda_x + \lambda_x^2}\right) \cdot \cdot \left[\lambda_x G_I \int_{t_0}^{t_1} (D - x_R)\, dt - v_L\lambda_v\right] \geq 0 \qquad (39)$$

It is necessary to know the condition by which (39) does not surpass the rest of the analyzed terms in order to make sure that $\dot{V}_{HO} \leq 0$. One way to do this is by relating this quantity with the term (37e).

$$x_R^2 \left[\frac{1}{2v_f}\lambda_v\lambda_x (\lambda_v + \lambda_x)^2\right] \geq \left(\lambda_v - \sqrt{\lambda_v^2 + \lambda_v\lambda_x + \lambda_x^2}\right) \cdot \cdot \left[\lambda_x G_I \int_{t_0}^{t_1} (D - x_R)\, dt - v_L\lambda_v\right] \qquad (40)$$

By using tne norm $||\cdot||_\infty$ in (40) it is possible to achieve

$$2\left\|\frac{x_R^2}{v_f}\right\|_\infty \geq \left(1 - \sqrt{3}\right)\left[G_I \| \int_{t_0}^{t_1} (D - x_R)\, dt\|_\infty - \|v_L\|_\infty\right] \qquad (41)$$

As early mentioned, integration term is non-positive. Therefore

$$\max\left(x_R^2\right) \geq \frac{\sqrt{3}-1}{2} \max\left(v_f\right) \max\left(v_L\right) \qquad (42)$$

By mechanical reasons, v_f and v_L are bounded. However, x_R can be increased without limit.

This last inequality (42) implies a condition for all the terms in (37), i.e. the combination of such terms gives a non-positive nature for such expression and then it is possible to conclude that

$$\dot{V}_{HO} \leq 0 \qquad (43)$$

and therefore, this control scheme is asymptotically stable.

4. CONCLUSION

Stability proofs for two models and two control schemes have been presented.

The first two stability proofs have been developed for the well-known Pipes' and Helly's Car-Following Models. The later is an extension of the former and such stability proofs are similar as expected.

The stability nature for both models is not only demonstrated as expected, but some interesting details have emerged, such as the way in which variables like v_f and x_R behave in real situations, supporting those analyses herein presented.

The stability proofs for those control designs presented in the original article of (Rosas-Jaimes et al., 2015) have been developed with the same matrices and quantities that appeared in such a paper. As for the models, interesting physical properties that match with the theoretical analyses herein presented in this work have been observed, supporting a realistic approach.

This document has had the only intention to show the stability proofs for all the models and control designs of those included in (Rosas-Jaimes et al., 2015). To this respect, this present work complements those results of this former article.

REFERENCES

W. Helly (1959) Simulation of Bottlenecks in Single Lane Traffic Flow. *Proceedings of the Symposium on Theory of Traffic Flow*, Research Laboratories, General Motors, Elsevier.

L. A. Pipes (1953) An Operational Analysis of Traffic Dynamics. *Journal of Applied Physics*, Vol. 24, No. 3, pp. 271–281.

O. A. Rosas-Jaimes, L. A. Quezada-Téllez, and G. Fernández-Anaya (2015). Control Design for Car-following Helly's Model. *Congreso Nacional de Control Automtico AMCA 2015*, pp. 293–298, October 14–16. Cuernavaca, Morelos, México, 2015.

M. Treiber, A. Hennecke and D. Helbing (2000). Congested traffic states in empirical observations and microscopic simulations. *Physical Review E*, 62 (2), pp. 1805–1824.